Isomers in the 'Merry-go-round' Process. Molecular *versus* Crystal Structure*

Dario Braga and Fabrizia Grepioni
Dipartimento di Chimica 'G. Ciamician', Università di Bologna, Via Selmi 2, 40126 Bologna, Italy

The relationship between crystal and molecular structure of the pairs of isomers in the 'merry-go-round' process $[Ir_4(CO)_9(\mu_3\text{-}\overline{SCH_2SCH_2SCH_2}\overline{)}]$ **1** and $[Ir_4(CO)_6(\mu\text{-}CO)_3(\mu_3\text{-}\overline{SCH_2SCH_2SCH_2}\overline{)}]$ **2**, and of the ionic species $[NMe_2(CH_2Ph)_2][Ir_4(CO)_{11}(SCN)]$ **3** and $[N(PPh_3)_2][Ir_4(CO)_8(\mu\text{-}CO)_3(SCN)]$ **4** has been investigated by means of atom–atom potential-energy calculations and packing analysis. It has been shown that in both **1** and **2** a network of weak C–H · · · O hydrogen-bonding interactions is established. In **2** these interactions involve only the bridging CO ligands. In **4** the cluster anions show a clear tendency to form anion piles surrounded by cation belts, while segregation of the SCN^- groups by the $NMe_2(CH_2Ph)_2^+$ cations has been observed in **3**. Tighter crystal packings are associated with the bridged isomers which also possess smaller molecular volumes than the all-terminal species.

In previous papers[1] we have investigated the relationship between the structure of neutral and ionic transition-metal clusters and the molecular organization in the solid state. In the cases of the high-nuclearity cluster anions based on the M_{10} (M = Ru or Os) tetracapped-octahedral metal framework or on the trigonal-prismatic M_6 framework (M = Co or Rh) a clear tendency to associate in anionic rows or piles surrounded by counter ions could be detected.[2a] Interestingly, the same packing motif found in crystals of the Os_{10} dianions was observed in the crystal of the neutral dihydride $[Os_{10}H_2C(CO)_{24}]$.[2b] More recently, we have investigated the relationship between molecular and crystal structure in the case of the polymorphs of $[Ru_6C(CO)_{17}]$.[3] The differences in molecular organization within the crystal have been related to the molecular flexibility involving the tricarbonyl units bound to the apical atoms in the structures of three independent molecules present in the two crystals. These studies were part of our continuing efforts towards the understanding of the packing modes of organometallic molecules[4] and of the dynamic processes occurring in crystals of mono- and poly-nuclear metal complexes.[5]

In an attempt to broaden this perspective further we now extend our approach to the study of some neutral and ionic clusters showing ligand isomerism in the solid state. To this purpose we have chosen to investigate the relationship between molecular and crystal structure in the case of isomeric iridium clusters **1**–**4** possessing tetrahedral metal frameworks, and for which two structural forms prevail in solution: 'all-terminal' with no bridging CO ligands and 'bridged' with three edge-bridging CO ligands spanning one tetrahedron face. These two forms have been shown by Cotton and co-workers[6] to be related through the so-called 'merry-go-round' carbonyl exchange process. The ligand frameworks of most M_4L_{12} clusters are structurally non-rigid in solution. The 'merry-go-round' interconversion between an all-terminal structure, as in $[Ir_4(CO)_{12}]$[7a] itself, and a bridged structure, as in $[Co_4(CO)_{12}]$,[7a,b] is the fundamental fluxional process leading to CO-scrambling in solution.[8]

The compound $[Ir_4(CO)_9(\mu_3\text{-}\overline{SCH_2SCH_2SCH_2}\overline{)}]$ has been shown to interconvert from one C_{3v} isomeric form with three edge-bridging CO groups around the cluster base bearing the trithiane ligand to a second C_{3v} form where all CO ligands are terminally bound.[9] The process is endothermic. More recently the results of a high-pressure ^{13}C NMR study of this species have been reported.[10] In this latter study the CO-exchange process was quantitatively characterized and the activation and reaction volumes for the interconversion process determined. In the solid state, depending on the temperature and on the crystallization solvents, both the 'ground-state' structure and the 'intermediate' one could be isolated and structurally characterized.[9] It has been shown that the structures of the bridged isomer (hereafter 'bridged-neutral' **2**) and of the all-terminal one (hereafter 'terminal-neutral' **1**) are closely related and differ essentially in the arrangement of the CO ligands and in the lengths of the Ir–Ir bonds (see also below).[9]

The second molecular pair chosen for this study is constituted by the cluster anions $[Ir_4(CO)_{11}(SCN)]^-$ and $[Ir_4(CO)_8(\mu\text{-}CO)_3(SCN)]^-$ which also exist in a bridged form (hereafter 'bridged anion' **4**) and in an all-terminal form (hereafter 'terminal anion' **3**) as shown. The two forms can be isolated in the respective crystalline salts depending on the counter ion choice: **4** as its $N(PPh_3)_2^+$ salt,[11a] and **3** as its $NMe_2(CH_2Ph)_2^+$ salt.[11b] In contrast to the trithiane derivatives, however, the fluxional process interconverting the two isomers has not (to the best of our knowledge) been studied by NMR methods although solid-state infrared spectra evidenced the presence of at least two different structural arrangements.[11b] In terms of solid-state molecular structure, beside the different distribution of the CO ligands, the two anions differ mainly in the orientation of the SCN group with respect to the cluster base and, as in the case of **1** and **2**, in the length of the metal-metal interactions.

In this study we will explore molecular and ion organization in the lattice of the two isomeric forms in order to see whether there is a recognizable packing control on the separation of the bridged and all-terminal structures. Furthermore an attempt will be made to relate deviations from idealized molecular symmetry to the effect on the individual molecular structure of the intermolecular force field. We have investigated the *crystal* structures of the species mentioned above by means of approximate packing potential energy calculations and (commonly available) molecular graphics software (see below). All necessary structural information was taken from the original diffraction studies. Our approach to crystal-packing problems is not conventional: the 'decoding' of the molecular or ion organization within the lattice is based on an analysis of the immediate neighbourhood of the reference ion (or molecule).

* *Supplementary data available* (No. SUP 56930, 2 pp.): Buckingham potential coefficients. See Instructions for Authors, *J. Chem. Soc., Dalton Trans.*, 1993, Issue 1, pp. xxiii–xxviii.

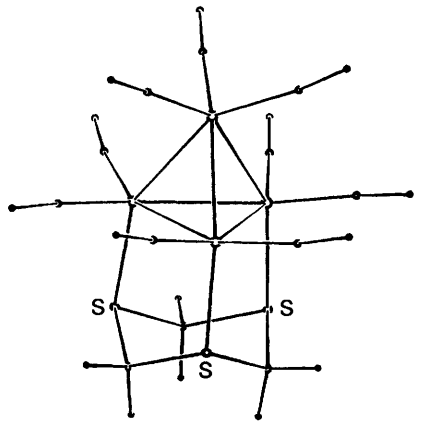

1

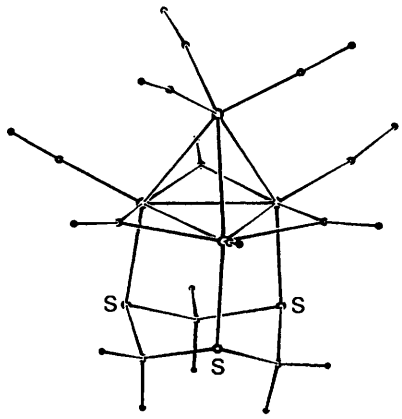

2

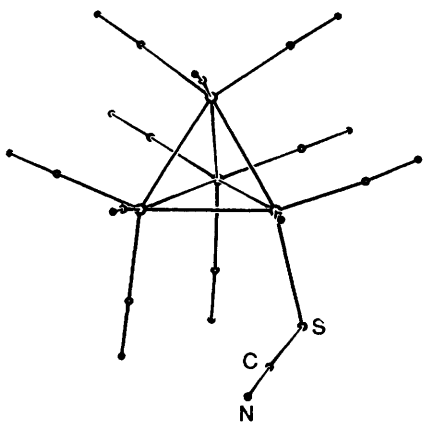

3

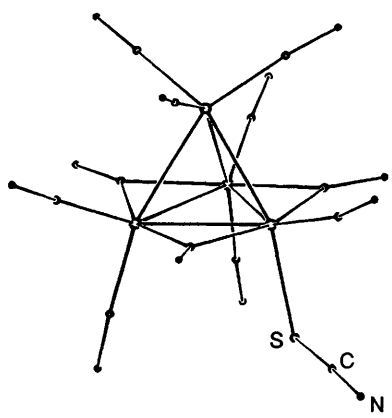

4

To this purpose we have developed a method based on atom–atom pairwise-potential-energy calculations,[12] and computer graphics. Use is made of the expression p.p.e. = $\Sigma_i\Sigma_j$-$[A\exp(-Br_{ij}) - Cr_{ij}^{-6}]$, where p.p.e. represents the packing potential energy, r_{ij} the non-bonded atom–atom intermolecular distance. Index i runs over all atoms of the reference molecule and j over the atoms of the surrounding molecules or ions within a preset cut-off distance (usually 15 Å). By this method the first co-ordination sphere around the reference cluster can easily be investigated and preferential packing motifs detected. Coulombic interactions due to the actual ionic charges in **3** and **4** were modelled by including in the summation a term of the kind q_iq_j/r_{ij}, where $q_{i,j}$ are point charges (see below). It should be stressed however that this procedure is used only in order to put on the same *relative* scale the p.p.e. values of the two ionic salts and not as a means to obtain reliable crystal potential-energy values. The volumes of the molecular or ionic units (V_{mol}, V_{anion}, V_{cation}) were calculated with the method of 'intersecting cups' of Kitaigorodsky by using literature van der Waals radii for main-group elements and an arbitrary radius of 2.35 Å for the Ir atoms; packing coefficients were estimated as p.c. = $V_{mol}Z/V_{cell}$. The calculation procedures of V_{mol} and p.c., as well as that of p.p.e., are all implemented within Gavezzotti's OPEC suite of programs;[13] SCHAKAL 88[14] was used for the graphical representation of the results.

The Molecular Structures

Since the molecular structures of the two trithiane derivatives **1** and **2** have already been described in a preliminary report[9] this section will only briefly summarize the main structural differences between the two species. Both isomers possess approximate C_{3v} symmetry. Isomer **1**, however, retains the all-terminal CO ligand distribution characteristic of $[Ir_4(CO)_{12}]$,[7a] while **2** possesses three bridging CO groups around the basal plane. This arrangement is common to most substitution derivatives of $[Ir_4(CO)_{12}]$ and recalls the C_{3v} structure of $[Co_4(CO)_9(\mu_3\text{-}CO)_3]$.[7b,c] Fig. 1(*a*) and 1(*b*) show views of the two molecular structures. Although both species possess an almost regular metal atom framework, Ir–Ir bonds are appreciably shorter in **1** than in **2** [range 2.633(1)–2.672(1) in **1**; 2.675(2)–2.690(2) in **2**; mean 2.655(1) *vs.* 2.683(2) Å][9] in agreement with the general observation that CO-bridge formation in Ir_4 (and Rh_4) clusters leads to lengthening of Ir–Ir bonding interactions.[15] Incidentally, the value of 2.655(1) Å is one of the shortest ever observed in substituted Ir_4 species. The trithiane ligands adopt a chair conformation and bind the three basal Ir atoms *via* two-electron Ir–S interactions. These interactions differ in length in the two molecules [mean 2.354(6) in **1**, 2.297(9) Å in **2**]. It is worth noting that the bridging CO group in **2** are markedly asymmetric. Although the Ir–C(bridge) interactions fall within the range 2.02(3)–2.18(3) Å, the 'short–long' bond sequence around the basal plane does not conform to the pseudo-three-fold symmetry of the molecule. The apical $(CO)_3$ unit is rotated *ca.* 16° from the orientation where Ir–C–O axes are *trans* to the base–apex Ir–Ir bonds. These appreciable deviations from idealized symmetry will be discussed in terms of inter- and intra-molecular non-bonding interactions in the following section.

The main structural difference between $[Ir_4(CO)_{11}(SCN)]^-$ and $[Ir_4(CO)_8(\mu\text{-}CO)_3(SCN)]^-$ [see Fig. 2(*a*) and 2(*b*)], beside the presence of bridging ligands and the lengthening of the basal Ir–Ir bonds, appears to originate from direct cation–anion interactions. The orientations of the SCN axis with respect to

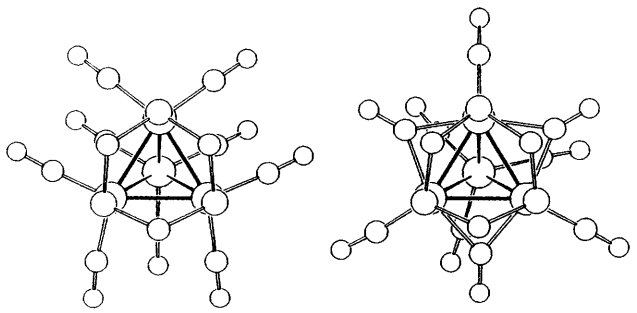

(*a*) (*b*)

Fig. 1 Projections perpendicular to the cluster basal plane of the molecular structure of the all-terminal (*a*) and bridged (*b*) isomers of $[Ir_4(CO)_9(\mu_3\text{-}SCH_2SCH_2SCH_2)]$ (species **1** and **2**, respectively). Note the torsion of the apical $(CO)_3$ unit and the asymmetry of the bridging CO groups in **2**

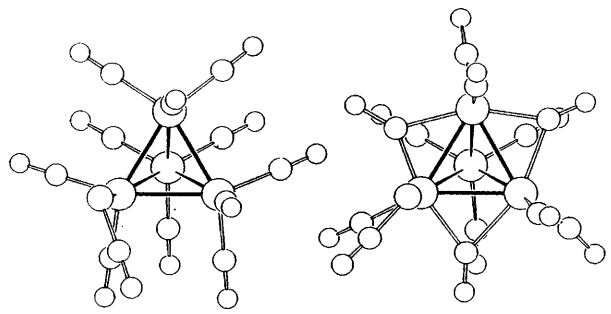

(*a*) (*b*)

Fig. 2 Projections perpendicular to the cluster basal plane of the structures of the all-terminal (*a*) and bridged (*b*) isomers of $[Ir_4(CO)_{11}(SCN)]^-$ (species **3** and **4**, respectively). Note the different orientations of the SCN^- group in the two molecular ions

the cluster base differ by about 60° in the two species. We will show in the following that this difference is very likely caused by the contact ion pair established with the two different counter ions. For more details on the anion structures the reader is addressed to the original papers.[11]

The Crystal Structures

All basic structural information and the values of some molecular and crystal parameters for all species discussed herein are summarized in Table 1. We will first discuss the molecular arrangement in crystalline **1** and **2** and then proceed by discussing the anionic species **3** and **4**.

Crystals of Complexes **1** *and* **2**.—The differences and similarities between the crystals of complexes **1** and **2** can be summarized as follows.

(*i*) The crystal packing of complex **2** is remarkably 'tight' with respect to **1** as reflected by the higher (calculated) density (3.98 *vs.* 3.72 g cm^{-3}, respectively). The packing coefficient is, however, identical (0.67) for the two crystals. This apparently contradictory behaviour is due to the smaller molecular volume of **2** with respect to **1** (324.8 *vs.* 347.4 $Å^3$, respectively).

(*ii*) The values of the packing potential energy (see Table 1) also indicate that the crystal packing of complex **2** is more cohesive by 37 kJ mol^{-1} (*ca.* 13%) than that of **1** (p.p.e.: 329 *vs.* 292 kJ mol^{-1}).

(*iii*) Intermolecular O · · · O and S · · · O contacts are shorter in complex **2** than in **1** (shortest O · · · O and O · · · S contacts: **2**, 2.87 and 3.09 Å; **1**, 3.22 and 3.44 Å, respectively). In particular, the O · · · O contacts in **2** are definitely much shorter than commonly observed in crystals of neutral carbonyl clusters (usually within the range 3.00–3.20 Å).[4c]

(*iv*) In keeping with the observation of a tight crystal packing for complex **2**, a comparison of the average atomic displacements in the two crystals indicates that all atomic species in **2** have less motional freedom than in **1** [U_{eq} averaged over the atomic species: Ir, 0.0081(6), 0.0196(4); S, 0.017(4), 0.040(3); C, 0.020(6), 0.038(5); O, 0.041(9), 0.073(7) $Å^2$ in **2** and **1**, respectively].

(*v*) The most striking feature of the two crystal packings is, however, the presence of a network of C–H · · · O hydrogen-bonding interactions between the carbonyl ligands and the H atoms of the trithiane groups. Although the positions of the H atoms were not observed in the X-ray experiments but calculated assuming 'regular' CH_2 geometry (*i.e.* H–C–H 109°, C–H 1.08 Å) the C–H · · · O interactions are easily detected on the basis of the length of the C(CH_2) · · · O(CO) separations which fall in the range 3.00–3.30 Å in **2** and 3.30–3.50 Å in **1**, *i.e.* towards the lower limit of the range commonly observed for C–H · · · O hydrogen bonds (3.00–4.00 Å).[16] The C–H · · · O distances less than 2.5 Å and related C–H · · · O and CO · · · H angular values for both species are reported in Table 2. Hydrogen bonds also appear as 'repulsions' in the partitioning of p.p.e. calculations over the individual groups of intermolecular interactions. This is because they bring the atoms involved below the actual van der Waals equilibrium distance, *i.e.* in the repulsive zone of the Buckingham potential. Fig. 3 shows the distribution of the **2** molecules in the 110 plane of the monoclinic lattice. The C–H · · · O distances below 2.5 Å involve exclusively the bridging CO groups and the trithiane ligands [O(9) · · · H(1), O(7) · · · H(6) and O(5) · · · H(4) are 2.29, 2.30 and 2.48 Å, respectively], while the terminal CO ligands do not appear to be involved in hydrogen bonding. Fig. 4 shows the C–H · · · O network in crystalline **1** (001 plane); the shortest C–H · · · O interaction (H · · · O 2.26 Å) 'links' the two independent molecules present in the triclinic lattice. In general, the shortest C–H · · · O distances appear to be associated with nearly linear interactions (see Table 2) in agreement with the trend observed in organic crystals.[16] We are not aware of previous observations of the existence of C–H · · · O interactions in crystals of typical organometallic clusters. In view of the large number of oxygen atoms covering the surface of the clusters, these interactions may play a far from negligible role in determining the actual packing choice (see below).

(*vi*) As mentioned above, the apical tricarbonyl unit in complex **2** is rotated *ca.* 16° from the '*trans*' position with respect to the apex–base Ir–Ir bonds [see Fig. 1(*b*)]. The presence on each sulfur atom of the trithiane ligand of one 'stereoactive' lone pair of electrons may be one of the reasons for the deviation from idealized geometry. Fig. 5 shows how two next-neighbouring molecules in the lattice of **2** interact: the apical tricarbonyl unit of molecule A is 'clamped' between one radial terminal CO and one S atom of molecule B, and the sulfur atom lone pair is very likely placed between two apical CO groups of the former molecule. It is, however, always difficult to discriminate between intra- and inter-molecular effects. The deformation could be due to steric interactions between the C atoms of the bridging CO groups and the apical ones. These interactions are alleviated by the torsion of the apical 'cone' away from exact eclipsing with the bridging ligands. Intramolecular apical–radial C · · · C contacts average 3.15 Å in the all-terminal **1** structure, while they decrease to 3.07 Å in **2** (a very simple calculation shows that these contacts decrease further to *ca.* 3.00 Å if the tricarbonyl unit is 'rotated back' into the idealized staggered position). However, one may object that a similar effect is not seen in **1**, nor is usually observed in CO-bridged derivatives of $[Ir_4(CO)_{12}]$. This difference is very likely due to the presence of the trithiane ligand underneath the cluster base which precludes downwards bending of the bridging CO groups as an alternative to $Ir(CO)_3$ torsion.

Crystals of Complexes **3** *and* **4**.—The most important structural relationships between the crystals of **3** and **4** will now be summarized.

Table 1 Relevant molecular and crystal parameters for $[Ir_4(CO)_9(\mu_3\text{-}SCH_2SCH_2SCH_2)]$ **1**, $[Ir_4(CO)_6(\mu\text{-}CO)_3(\mu_3\text{-}SCH_2SCH_2SCH_2)]$ **2**, $[NMe_2(CH_2Ph)_2][Ir_4(CO)_{11}(SCN)]$ **3**, and $[N(PPh_3)_2][Ir_4(CO)_8(\mu\text{-}CO)_3(SCN)]$ **4**

Species	Crystal system	Space group	Z	V_{cell}	V_{unit}	V_{mol}	p.c.	p.p.e.
2	Monoclinic	Cc	4	1934(1)	483.5	324.8	0.67	−329
1	Triclinic	$P\bar{1}$	4	2067(2)	516.8	347.4[a]	0.67	−292
						V_{anion}, V_{cation}		
4	Monoclinic	$P2_1/a$	4	5095	1273.8	312.3, 508.5	0.64	−408,[b] −658,[c] −606[d]
3	Monoclinic	$P2_1/c$	4	3506(2)	876.5	335.2, 240.1	0.66	−394,[b] −532,[c] −448[d]

V_{cell}, V_{unit} (volume of the asymmetric unit), V_{mol}, V_{anion}, V_{cation} in Å^3; p.p.e. in kJ mol^{-1} (see SUP 56930 for the values of the coefficients A, B and C used for the calculations of p.p.e.). [a] Averaged over the volumes of the two independent molecular units (347.2 and 347.7 Å^3, respectively). [b] No Coulombic term. [c] Coulombic term with negative charge on the S atoms, positive charge on the central atom of the cation. [d] Coulombic term with negative charge on the centre of mass of the anion, positive charge on the central atom of the cation.

Table 2 Relevant structural parameters of the C–H · · · O interactions (distances in Å, angles in °)

Isomer **2**					
O(9) · · · H(1)	2.29	O(9) · · · H(1)–C(10)	167.0	C(9)–O(9) · · · H(1)	169.4
O(7) · · · H(6)	2.30	O(7) · · · H(6)–C(12)	124.7	C(7)–O(7) · · · H(6)	170.7
O(5) · · · H(4)	2.48	O(5) · · · H(4)–C(11)	123.9	C(5)–O(5) · · · H(4)	160.3
Isomer **1**					
O(2) · · · H(8)	2.38	O(2) · · · H(8)–C(22)	155.5	C(2)–O(2) · · · H(8)	154.8
O(4) · · · H(9)	2.34	O(4) · · · H(9)–C(23)	167.1	C(4)–O(4) · · · H(9)	153.3
O(7) · · · H(3)	2.40	O(7) · · · H(3)–C(11)	159.1	C(7)–O(7) · · · H(3)	156.1
O(9) · · · H(11)	2.43	O(9) · · · H(11)–C(24)	156.7	C(9)–O(9) · · · H(11)	154.7
O(20) · · · H(1)	2.40	O(20) · · · H(1)–C(10)	135.0	C(20)–O(20) · · · H(1)	154.9
O(15) · · · H(5)	2.26	O(15) · · · H(5)–C(12)	166.6	C(15)–O(15) · · · H(5)	166.4
O(18) · · · H(2)	2.45	O(18) · · · H(2)–C(10)	134.9	C(18)–O(18) · · · H(2)	133.8

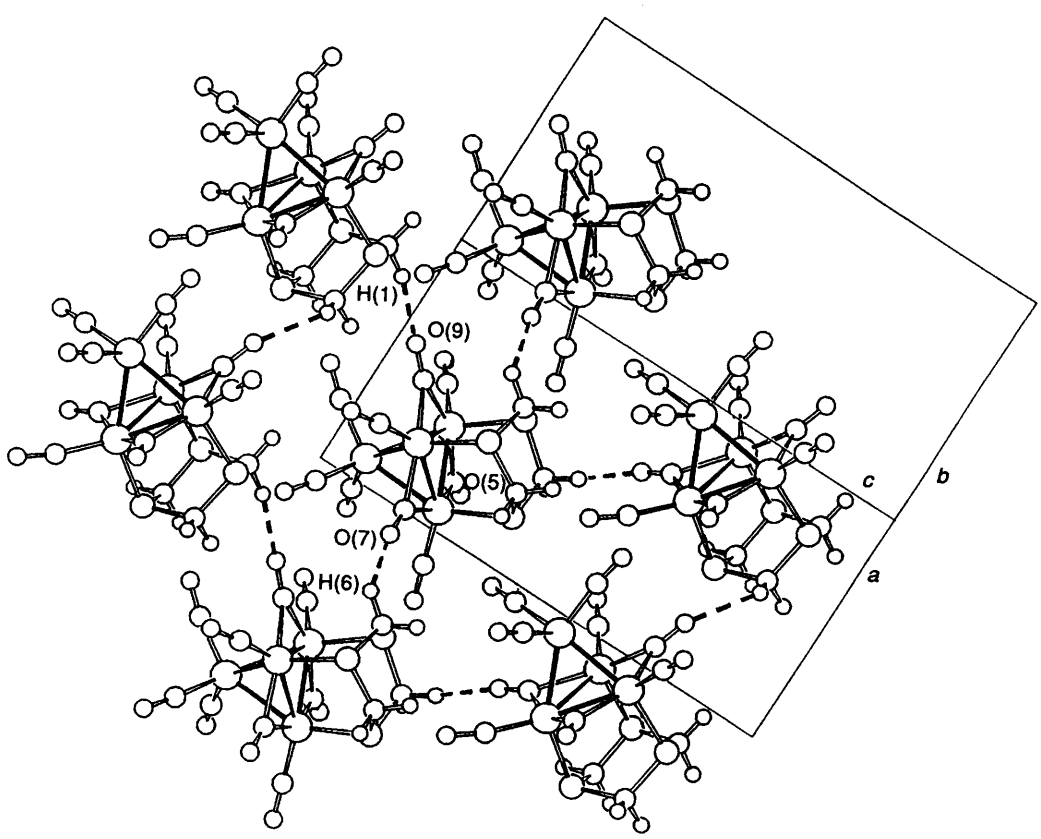

Fig. 3 Molecular distribution in the 110 lattice plane of complex **2**, showing the network of C–H · · · O interactions (only those shorter than 2.5 Å are shown as broken bonds). The O(5) · · · H(4) interactions are not shown, for sake of clarity, because they link molecules above and below the plane

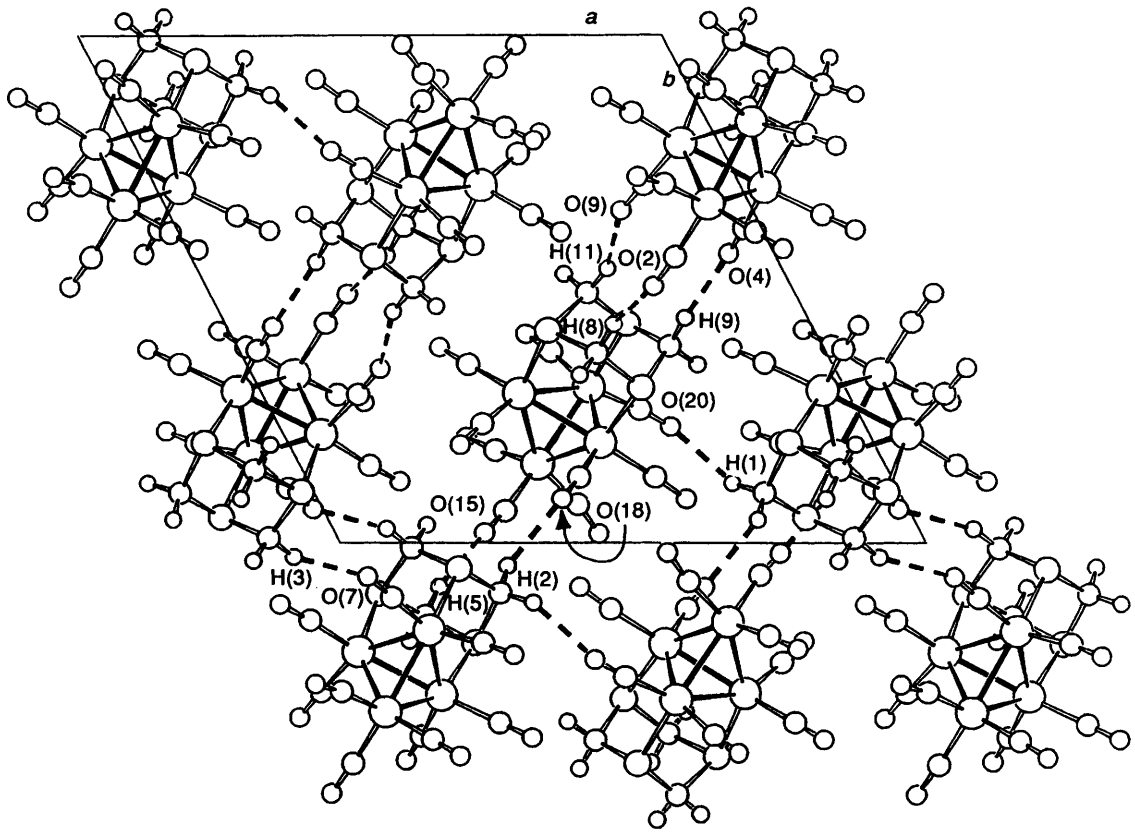

Fig. 4 Molecular distribution in the 001 lattice plane of complex **1**, showing the network of C–H · · · O interactions shorter than 2.5 Å. The shortest such bonds (2.26 Å) link the two crystallographically independent molecules

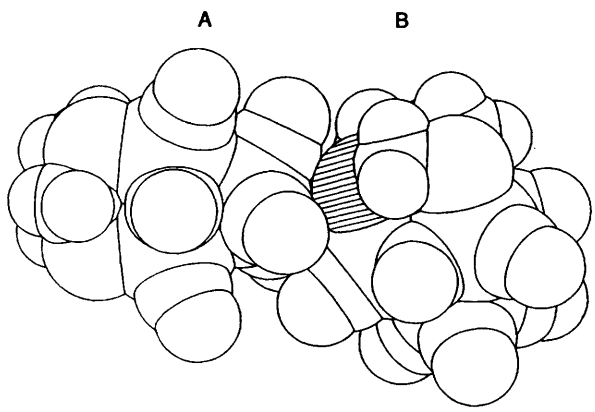

Fig. 5 The interaction between two next-neighbouring molecules in the lattice of complex **2**, showing how the apical tricarbonyl unit of molecule A is 'clamped' between the S-atom lone pair and one basal CO of the molecule B

(*i*) In contrast to the pair **1** and **2**, no significant differences in intermolecular contacts with the surrounding ions can be detected in the two crystal packings.

(*ii*) The pseudo-radial SCN orientation in complex **4** affects the other axial CO groups, which appear 'pushed away' from the sulfur side [see Fig. 2(*b*)], while similar deformation is not observed in **3** [intramolecular S · · · C(CO) contacts are *ca.* 3.65 Å in **4** and 3.40 Å in **3**]. We believe this to be a consequence of the stereoactive effect of the S-atom lone pairs which in **4** are oriented *towards* the axial CO groups, while they 'interfere' much less with the other axial ligands in **3**. It is not possible to say, however, whether this effect arises because the counter ion favours a specific SCN orientation (which then causes the axial CO groups to be pushed away, metal–metal bonds to lengthen and bridging CO groups to be established in order to compensate for loss of metal–metal bonding overlap)[15] or because the CO-fluxionality process causes continuous shrinking and swelling of the cluster core ('breathing motion') which is accompanied by rotation (or swinging motion) of the SCN^- group about the Ir–S axis. In this latter hypothesis it would appear that it is the actual counter ion that 'traps' one of the possible SCN orientations at the nucleation stage. The ligands are then 'locked in place' in their respective lattices without rotational freedom {as expected, rotation of the SCN^- group about the Ir–S bond in **4** in order to achieve the same orientation as seen in **3** [compare Fig. 2(*a*) and 2(*b*)] gives rise to extremely short contacts with the surrounding cations}.

(*iii*) Since the volume of the $N(PPh_3)_2^+$ cation is more than twice that of $NMe_2(CH_2Ph)_2^+$ (508.5 *vs.* 240.1 $Å^3$) the ratio in size between the anion and cation is very different in complexes **3** and **4**. In crystalline **3** the $NMe_2(CH_2Ph)_2^+$ cation is much smaller than the cluster anion, while the situation reverts with $N(PPh_3)_2^+$ in **4** (V_{anion}/V_{cation} = 335.2/240.1 = 1.4 *versus* 312.3/508.5 = 0.61). The volumes of the cations compare well with the values reported recently in a study of the crystal packing of some inorganic salts.[17] Although the volumes calculated on the basis of the Kitaigorodsky 'intersecting cups' model are, in general, slightly bigger than the value obtained with Gavezzotti's integration model, the differences do not appear to be significant within the context of this analysis.

(*iv*) The difference in size between the two cations is reflected in the difference in p.p.e. values (see Table 1): the p.p.e. is *ca.* 12 kJ mol^{-1} (*ca.* 6%) more cohesive in complex **4** than in **3**. This is not to say that large cations give more stable crystals than small ones, rather we note that, as in the case of the pair **1** and **2**, the most cohesive packing is associated with the bridged isomer. This difference is maintained when the Coulombic term is included in the calculation (see Table 1).

(*v*) The lattice of complex **3** is essentially built around 'dimeric units' formed by pairs of cluster anions (see Fig. 6).

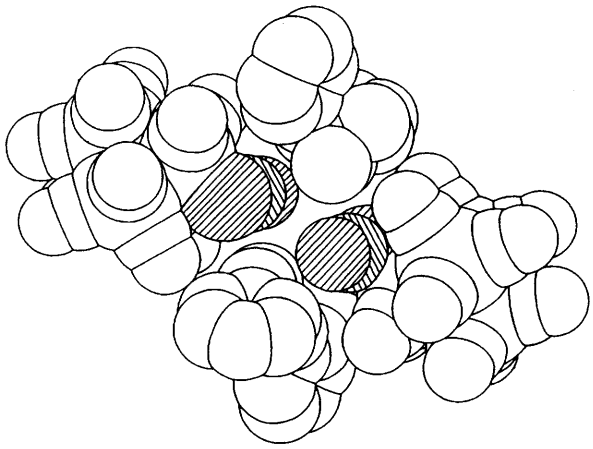

Fig. 6 The 'dimeric' unit formed by pairs of **3** anions; the SCN^- groups are placed in antiparallel mode and are 'trapped' among four cations. For sake of clarity only two $NMe_2(CH_2Ph)_2^+$ cations are shown, the other two being placed above and below the plane completely enclosing the SCN^- groups

(*a*)

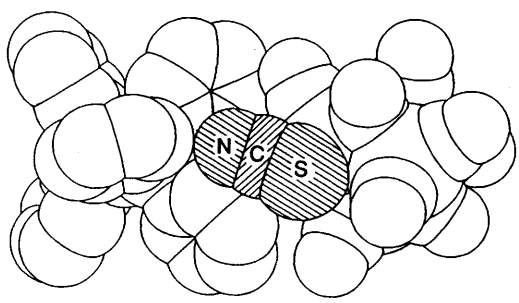

(*b*)

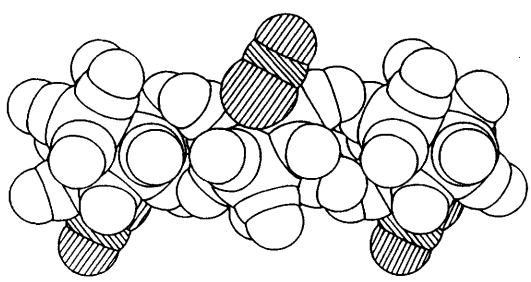

Fig. 7 (*a*) The cation–anion interaction in crystalline complex **4**: the SCN^- group points towards the $N(PPh_3)_2^+$ cation. (*b*) One row of anions extending along the *c* axis

The two SCN groups are placed anti-parallel and appear to point the free N end towards the centre of the $NMe_2(CH_2Ph)_2^+$ cation. Direct cation–anion interaction is observed with the SCN^- groups 'segregated' among four counter ions. For this reason the SCN^- group appears to carry the negative charge, while the remaining part of the molecular ion behaves as if essentially neutral interacting with neighbouring anions in van der Waals fashion *via* CO · · · CO interlocking as observed with neutral molecules.[1]

(*vi*) Direct SCN^-–cation interactions are clearly recognizable also in crystalline complex **4**, in spite of the presence of the large $N(PPh_3)_2^+$ cation [see Fig. 7(*a*)]. In this lattice, however, the anions self-organize in piles throughout the crystal lattice, with the piles extending parallel to the crystallographic *c* axis [see Fig. 7(*b*)]. It is noted that the SCN^- groups point outward along the cluster pile in an alternating fashion; each SCN^- group (as in **3**) interacts directly with the neighbouring $N(PPh_3)_2^+$ cation, directing the nitrogen terminus towards one of the P atoms as shown in Fig. 7(*a*).

Conclusion

With this paper we have attempted, in a sense, to address the perpetual steric–electronic dualism which controls the 'final' geometry (or geometries) that a molecule can possess in the solid state. It is worth stressing that this dualism pervades all aspects of structural chemistry not merely the study of molecular solids. Perhaps we have not been able to find appropriate answers to all questions listed in the Introduction, nonetheless we believe some of the unexpected findings have made this analysis worthwhile.

The difference in van der Waals volumes between unbridged and bridged species for each isomeric pair is identical (*ca.* 23 $Å^3$) irrespective of the presence of different ligands. This is only apparently in contrast with what one might expect on the basis of the difference in metal cluster size (Ir–Ir bonds are longer in **2**,**4** than in **1**,**3**, see above) because the bridging C atoms in **2**,**4** are embedded within the iridium co-ordination spheres and contribute much less to the molecular volumes. In this respect, it is worth stressing that the higher molecular density of **2** with respect to **1** is in agreement with the positive activation volume obtained by variable-pressure NMR spectroscopy for the **2** ⟷ **1** interconversion process. Although great caution must be exerted on quantitative comparison of p.p.e. values obtained for large organometallic molecules, we note that the most cohesive crystals are associated with the bridged species of both isomeric pairs (intermolecular hydrogen bonds also favouring **2** with respect to **1** [16]). Since, at least in the case of the trithiane derivatives, the bridged species corresponds to the 'ground-state' structure, while the unbridged is an intermediate, we might argue that the isolation of this latter species in crystalline form is mainly under kinetic control.

There are structural features that can be accounted for in terms of intramolecular interactions: the torsion of the apical tricarbonyl unit in complex **2** is most likely due to repulsions between the bridging ligands and the apical ones. Similarly, in **4** and **3** the stereoactivity of the S-atom lone pairs is clearly recognizable and the orientation of the SCN^- group affects the molecular geometry.

In terms of intermolecular interactions the neutral trithiane derivatives clearly show the presence of a network of C–H · · · O hydrogen bonds (see below). In **2** only the bridging CO ligands, which are the most basic carbonyls in the structure, are involved in short hydrogen bonds. These interactions affect the molecular geometry and appear to be responsible for the asymmetry of the CO bridges, i.e. for the deviation of the molecular geometry observed in the solid state from the idealized C_{3v} molecular symmetry.

In the anionic species the negative charge appears to be carried by the SCN^- groups. These ligands establish evident contact-pair interactions in both crystalline environments. In complex **3** the ligands are segregated within a 'cage' generated by four surrounding $NMe_2(CH_2Ph)_2^+$ cations, while in **4** the formation of anionic piles, previously observed in other high-nuclearity crystalline salts,[2a] is found again. The $N(PPh_3)_2^+$ cation, which is very large and capable of 'folding' around the cluster anions, appears to assist the formation of one-dimensional anion arrays within the three-dimensional lattice. We can anticipate here that, in the case of octahedral cluster salts, similar structural relationships between size and flexibility of the cations and ion organization have been observed and will be the subject of a forthcoming paper.

Another example of cation-dependent molecular structure in the solid state is that of $[Fe_4(CO)_{13}]^{2-}$.[18] The dianion possesses a slightly distorted all-terminal structure in its $N(PPh_3)_2^+$ salt,[18a] while the earlier reported $[Fe(py)_6]^{2+}$ (py = pyridine) salt shows the anion to possess asymmetric bridging CO groups.[18b] This difference was taken as indicative of a small

energy difference between the two structures. Together with the structures of the neutral mixed-metal analogue $[FeCo_3H(CO)_9\{P(OMe)_3\}_3]$,[18c] these molecules were regarded[18a] as belonging to the same CO-ligand interconversion pathway. A similar structural correlation between solution behaviour and solid-state geometry is shown by the family of 13-CO clusters $[Co_6C(CO)_{13}]^{2-}$,[19a] $[Rh_6C(CO)_{13}]^{2-}$,[19b] and $[Co_2Rh_4C(CO)_{13}]^{2-}$.[19c] The latter mixed-metal species shows a CO-ligand distribution which is intermediate between those possessed by the two homometallic clusters.

The role of the C–H · · · O interactions (if not their very existence as a 'special type' of intermolecular interactions) has been the subject of much debate mainly in the organic solid-state chemistry field. A very good account of this, as well as a definitive identification of these interactions as weak hydrogen bonds has recently been published by Desiraju.[16] The C–H · · · O bonds have been termed 'tug-boat' or 'steering' forces since, though weak, they appear to be capable of driving the crystallization process towards one particular pathway. It may well be that in organometallic crystals, where a large number of CO groups are often present, these interactions have a far from negligible effect on the crystallization process and stability. Intermolecular C–H · · · O networks have also been observed in crystalline formylferrocene $[Fe(C_5H_5)(C_5H_4COH)]$[20a] and in the crystal of the cyanocarbene derivative $[Fe_2(C_5H_5)_2(CO)_3\{HC(CN)\}]$.[20b]

Finally, we have shown that, in discussing the solid-state structure of non-rigid (fluxional) organometallic molecules, it is paramount always to keep in mind that the whole set of 'bonding' (electronic) and 'non-bonding' (steric) *intramolecular* interactions, responsible for the actual molecular geometry, is embedded in the *intermolecular* force field responsible for crystal stability. In particular, when intermolecular interactions are in competition with finely balanced intramolecular interactions (both of bonding and non-bonding nature) the effect on the actual molecular geometry might be difficult to predict. Hence, the solid-state molecular structures of flexible organometallic molecules ought always to be discussed within the environment in which they belong.

Acknowledgements

Financial support by Ministero della Universitá e della Ricerca Scientifica e Technologica is acknowledged. We thank A. G. Orpen for useful comments.

References

1 D. Braga and F. Grepioni, *Organometallics*, 1991, **10**, 1254; D. Braga, F. Grepioni, B. F. G. Johnson, J. Lewis, C. E. Housecroft and M. Martinelli, *Organometallics*, 1991, **10**, 1260.
2 (*a*) D. Braga and F. Grepioni, *Organometallics*, 1992, **11**, 1256; (*b*) D. Braga, F. Grepioni, S. Righi, B. F. G. Johnson, P. Frediani, M. Bianchi, F. Piacenti and J. Lewis, *Organometallics*, 1991, **10**, 706.
3 D. Braga, F. Grepioni, B. F. G. Johnson, P. Dyson, P. Frediani, M. Bianchi, F. Piacenti and J. Lewis, *J. Chem. Soc., Dalton Trans.*, 1992, 2565.
4 (*a*) D. Braga and F. Grepioni, *Organometallics*, 1991, **10**, 2563; (*b*) D. Braga and F. Grepioni, *Organometallics*, 1992, **11**, 711; (*c*) D. Braga, F. Grepioni and P. Sabatino, *J. Chem. Soc., Dalton Trans.*, 1990, 3137; (*d*) D. Braga, F. Grepioni, A. Gavezzotti and P. Sabatino, *J. Chem. Soc., Dalton Trans.*, 1992, 1185.
5 D. Braga, *Chm. Rev.*, 1992, **92**, 633.
6 F. A. Cotton, *Inorg. Chem.*, 1966, **5**, 1083; J. G. Bullit, F. A. Cotton and T. J. Marks, *J. Am. Chem. Soc.*, 1970, **92**, 2155.
7 (*a*) M. R. Churchill and J. P. Hutchinson, *Inorg. Chem.*, 1978, **17**, 5328; (*b*) C. H. Wei, *Inorg. Chem.*, 1969, **8**, 2384; (*c*) F. H. Carre, F. A. Cotton, B. A. Frenz, *Inorg. Chem.*, 1976, **15**, 380.
8 F. A. Cotton and B. E. Hanson, *Rearrangements in Ground and Excited States*, ed. P. De Mayo, Academic Press, New York, 1980, p. 379; S. Aime and L. Milone, *Prog. Nucl. Magn. Reson. Spectrosc.*, 1977, **11**, 183.
9 G. Suardi, A. Strwczynski, R. Ros, R. Roulet, F. Grepioni and D. Braga, *Helv. Chim. Acta*, 1990, **73**, 154.
10 A. Orlandi, U. Frey, G. Suardi, A. E. Merbach and R. Roulet, *Inorg. Chem.*, 1992, **31**, 1304.
11 (*a*) R. Della Pergola, L. Garlaschelli, S. Martinengo, F. DeMartin, M. Manassero and M. Sansoni, *Gazz. Chim. Ital.*, 1987, **117**, 245; (*b*) M. P. Brown, D. Burns, M. M. Harding, S. Maginn and A. K. Smith, *Inorg. Chim. Acta*, 1989, **162**, 287.
12 A. J. Pertsin and A. I. Kitaigorodsky, *The Atom–Atom Potential Method*, Springer, Berlin, 1987; A. Gavezzotti and M. Simonetta, *Chem. Rev.*, 1981, **82**, 1; K. Mirsky, *Proceedings of the International Summer School on Crystallographic Computing*, Delft University Press, Twente, 1978, p. 169.
13 A. Gavezzotti, OPEC, *Organic Packing Potential Energy Calculations*, University of Milano, 1982; see also A. Gavezzotti, *J. Am. Chem. Soc.*, 1983, **195**, 5220.
14 E. Keller, SCHAKAL 88, *Graphical Representation of Molecular Models*, University of Freiburg, 1988.
15 D. Braga and F. Grepioni, *J. Organomet. Chem.*, 1987, **336**, C9.
16 G. R. Desiraju, *Acc. Chem. Res.*, 1991, **24**, 290.
17 D. M. P. Mingos and A. R. Rohl, *J. Chem. Soc.. Dalton Trans.*, 1991, 3419; *Inorg. Chem.*, 1991, **30**, 3769.
18 (*a*) G. Van Buskirk, C. B. Knobler and H. D. Kaesz, *Organometallics*, 1985, **4**, 149; (*b*) R. J. Doedens and L. F. Dahl, *J. Am. Chem. Soc.*, 1978, **100**, 3059.
19 (*a*) V. G. Albano, D. Braga and S. Martinengo, *J. Chem. Soc., Dalton Trans.*, 1986, 981; (*b*) V. G. Albano, D. Braga and S. Martinengo, *J. Chem. Soc., Dalton Trans.*, 1981, 717; (*c*) V. G. Albano, D. Braga, F. Grepioni, R. Della Pergola, L. Garlaschelli and A. Fumagalli, *J. Chem. Soc., Dalton Trans.*, 1989, 879, 981.
20 (*a*) K. Sato, M. Iwai, H. Sano and M. Konno, *Bull. Soc. Chem. Jpn.*, 1984, **57**, 634; (*b*) S. Aime, L. Cordero, R. Gobetto, S. Bordoni, L. Busetto, V. Zanotti, V. G. Albano, D. Braga and F. Grepioni, *J. Chem. Soc., Dalton Trans.*, 1992, 2961.

Received 2nd November 1992; *Paper* 2/05846D